Dark Matter

ASTR 333/433
Fall 2013
MoTu 4:00-5:15pm
Sears 552

Prof. Stacy McGaugh
Sears 573
368-1808
stacy.mcgaugh@case.edu

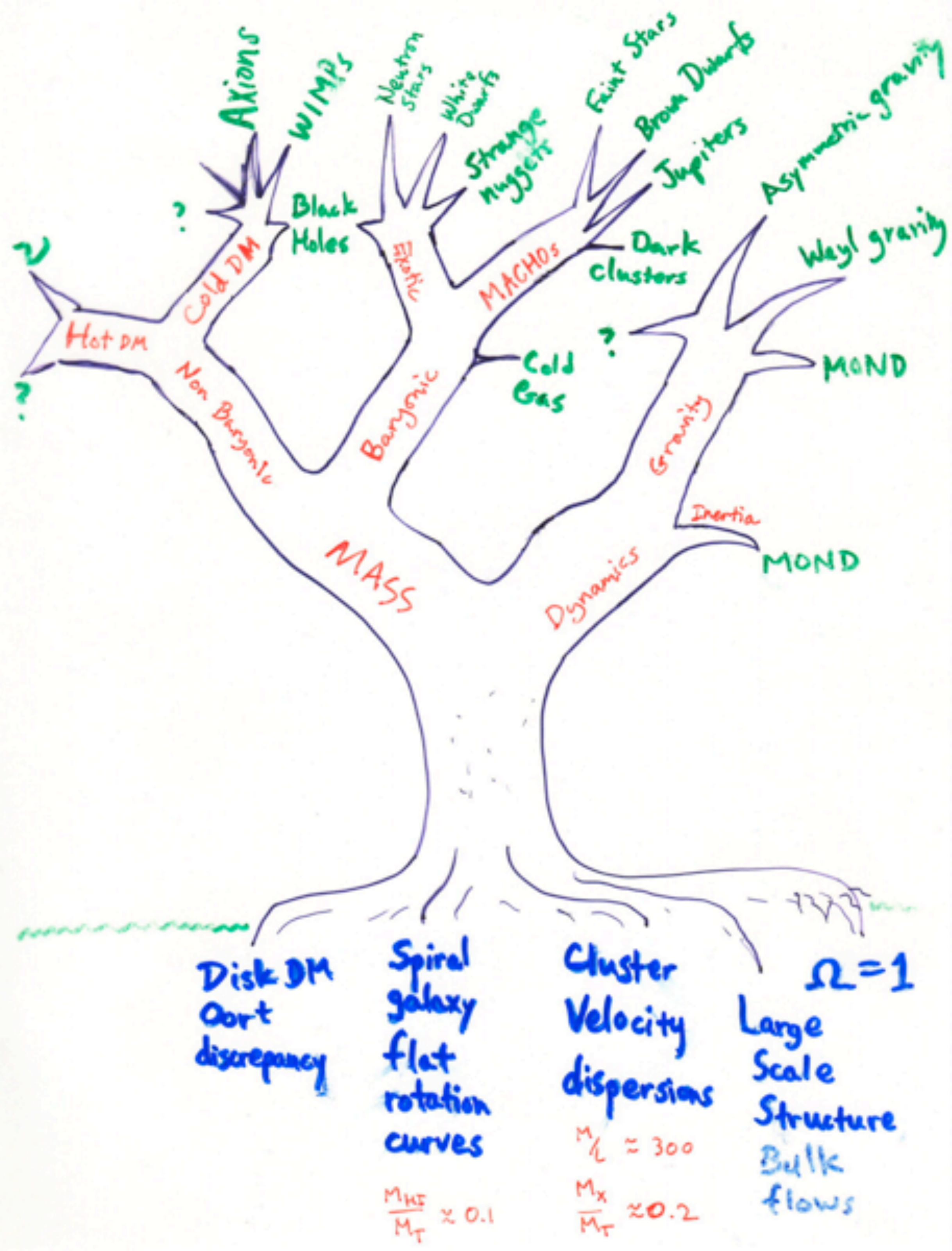

Case Western Reserve University EST. 1826

Logistics:

- Homework 3 due tomorrow
- Abstracts for 433 talks due 11/26
- 433 talks 12/2 & 12/3
- Homework 4 due 12/3
- Review 12/9
- Final 12/11 (9 AM)

Today: cluster masses from

- X-ray gas
- S-Z effect

Galaxy Clusters

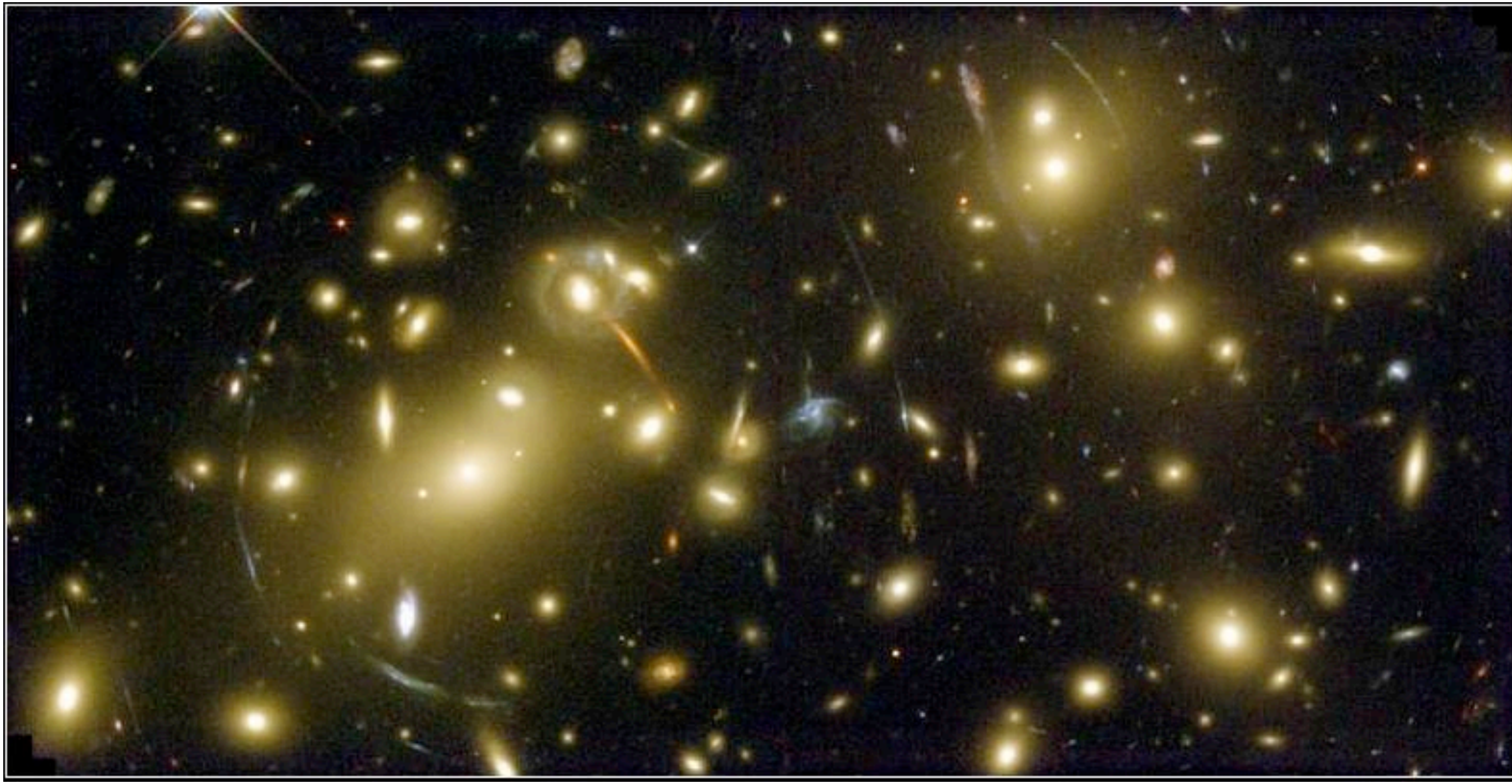

4 distinct measures: velocity dispersion, gravitational lensing, hydrostatic equilibrium of X-ray gas, and the Sunyaev-Zel'dovich effect

Clusters in optical and X-ray (contours)

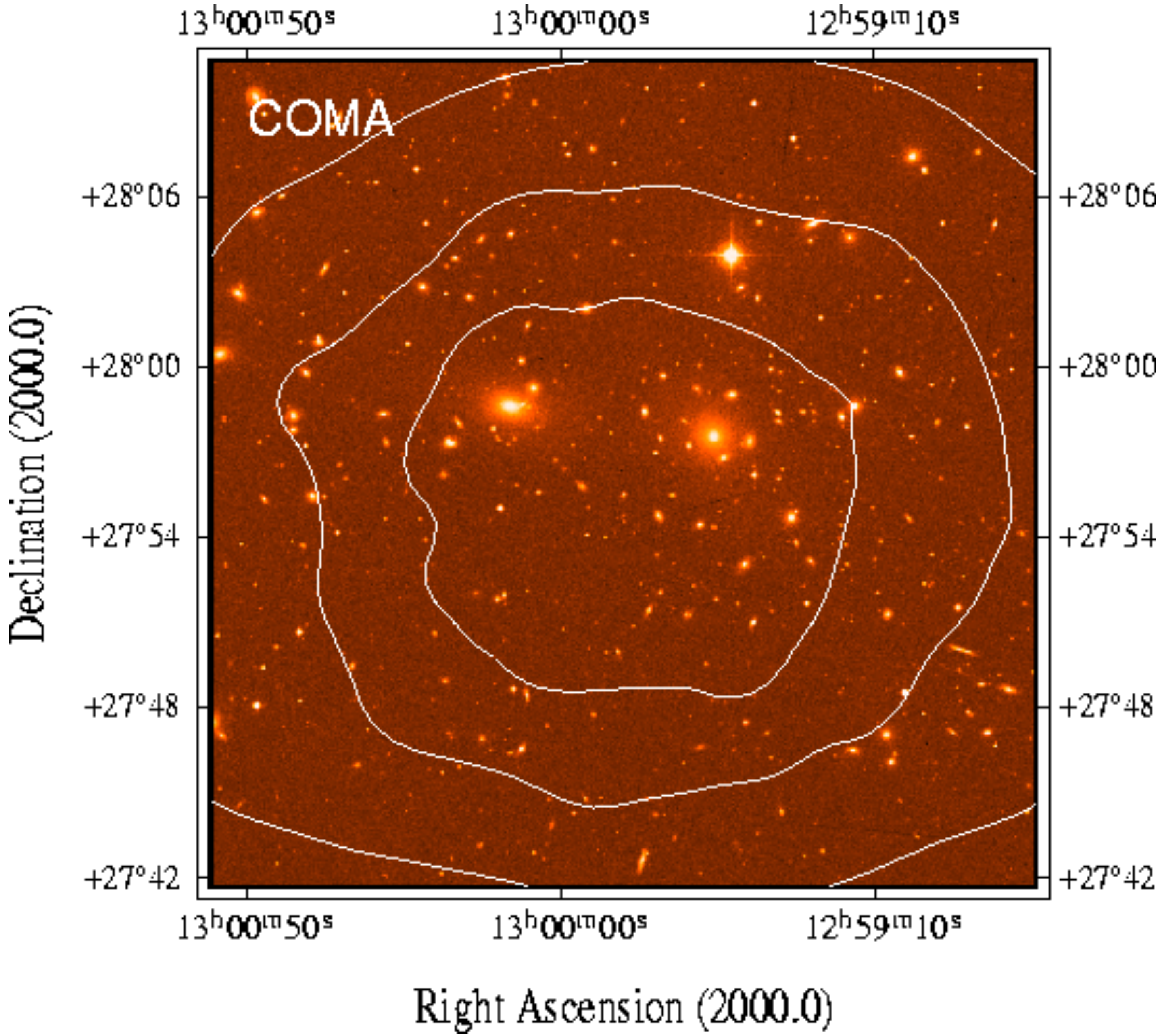

Reiprich ApJ, 567, 716-740 (2002)

Clusters in optical and X-ray (contours)

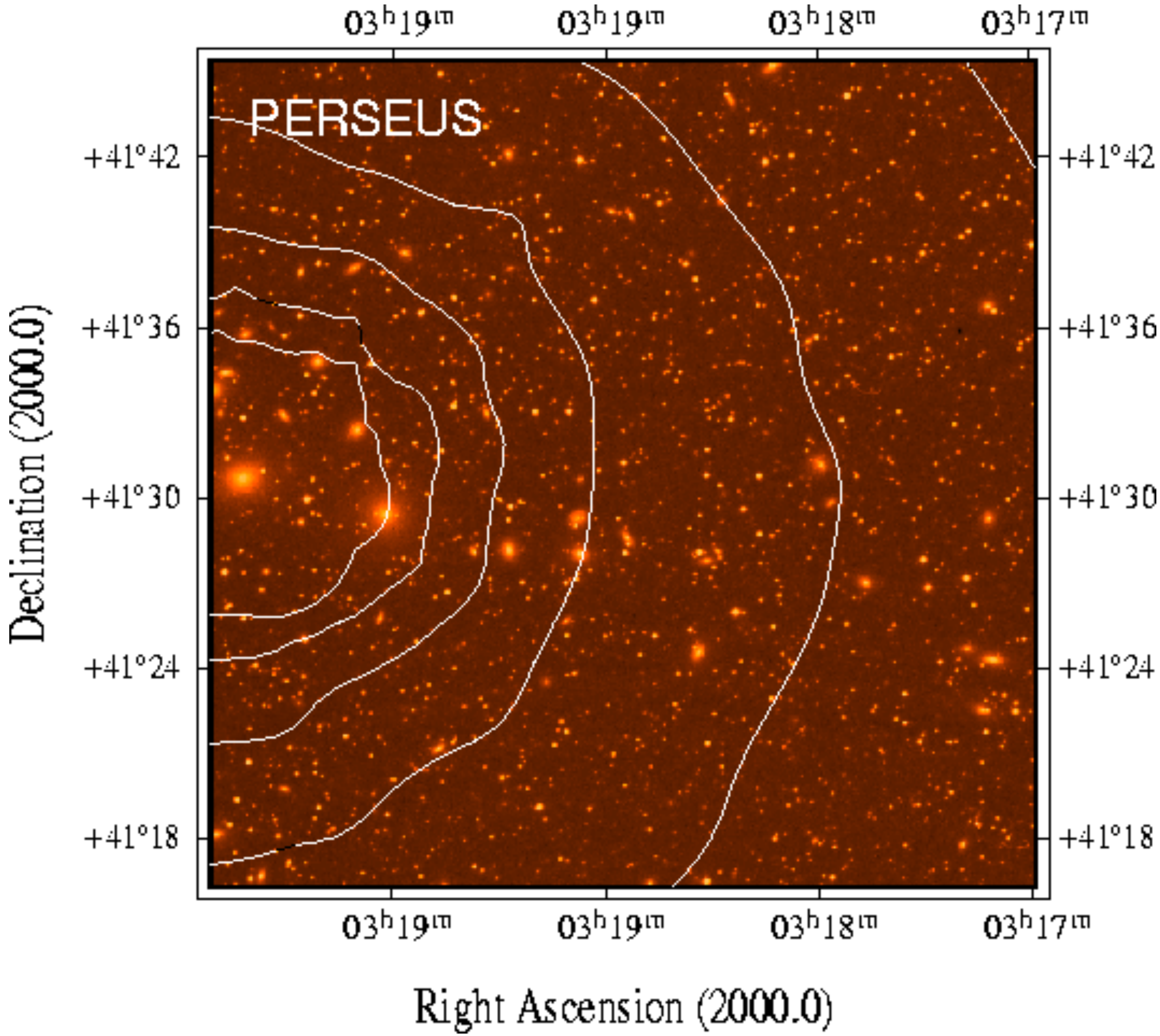

Reiprich ApJ, 567, 716-740 (2002)

Clusters in optical and X-ray (contours)

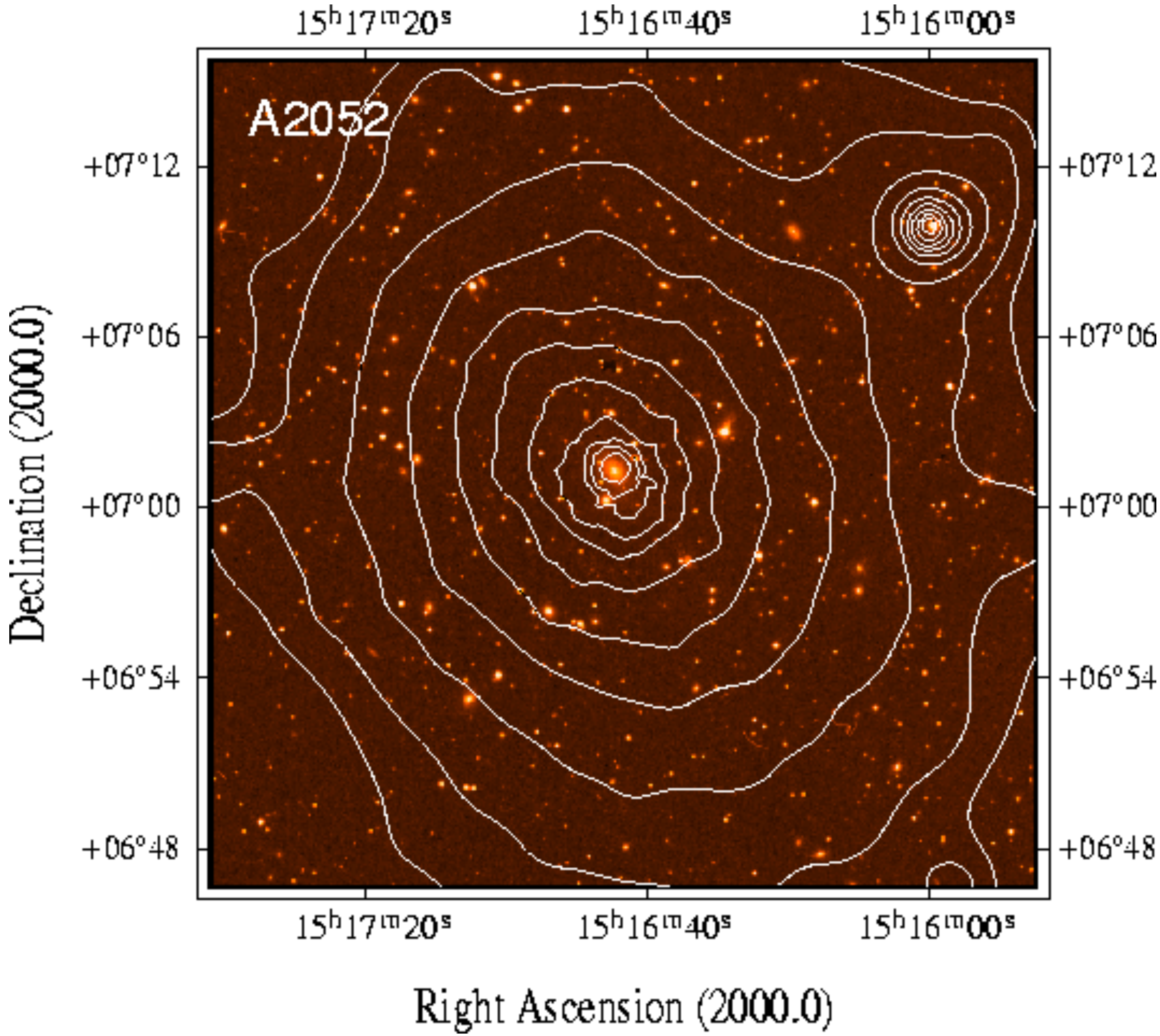

Reiprich ApJ, 567, 716-740 (2002)

Clusters in optical and X-ray (contours)

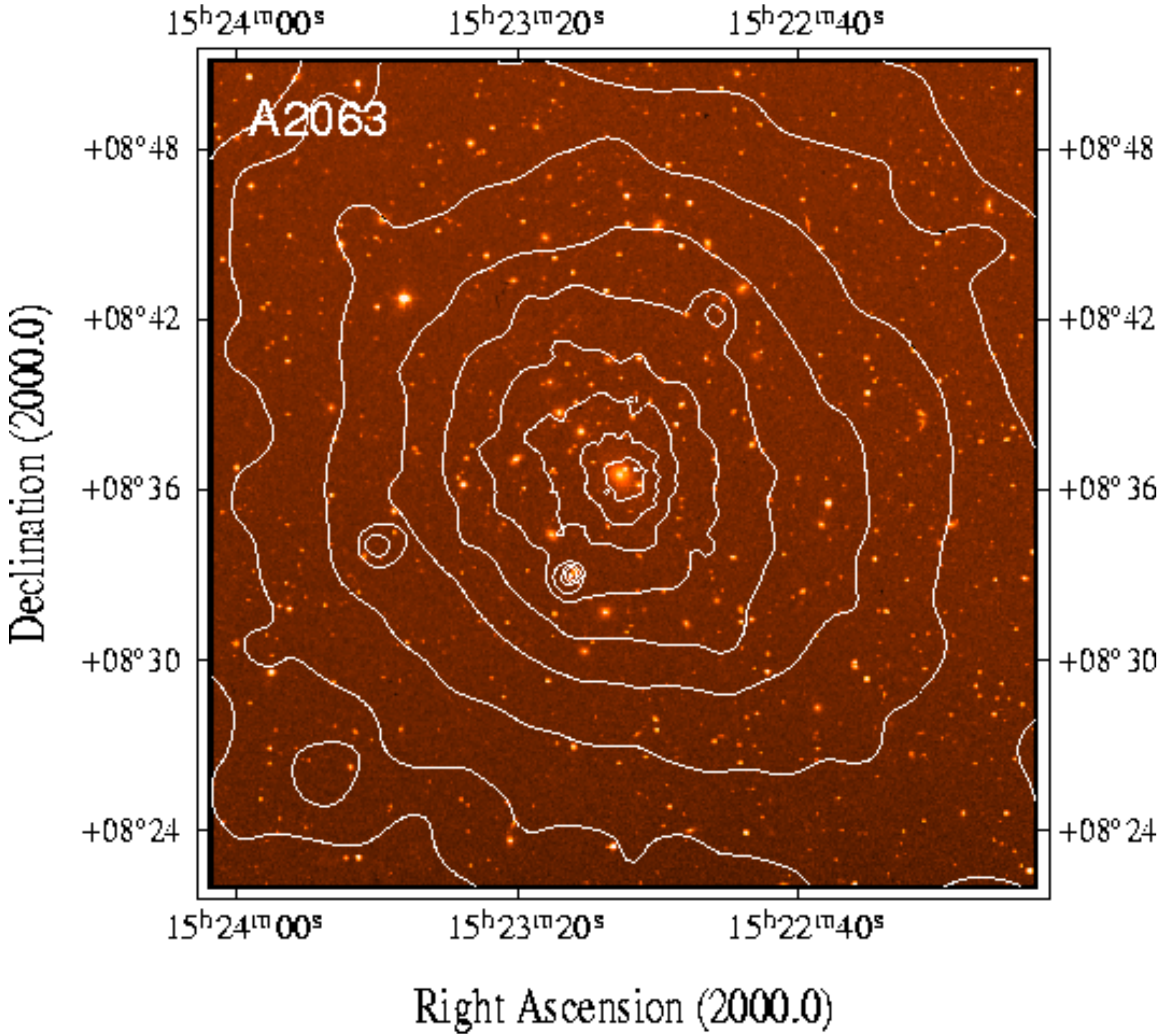

Reiprich ApJ, 567, 716-740 (2002)

Clusters in optical and X-ray (contours)

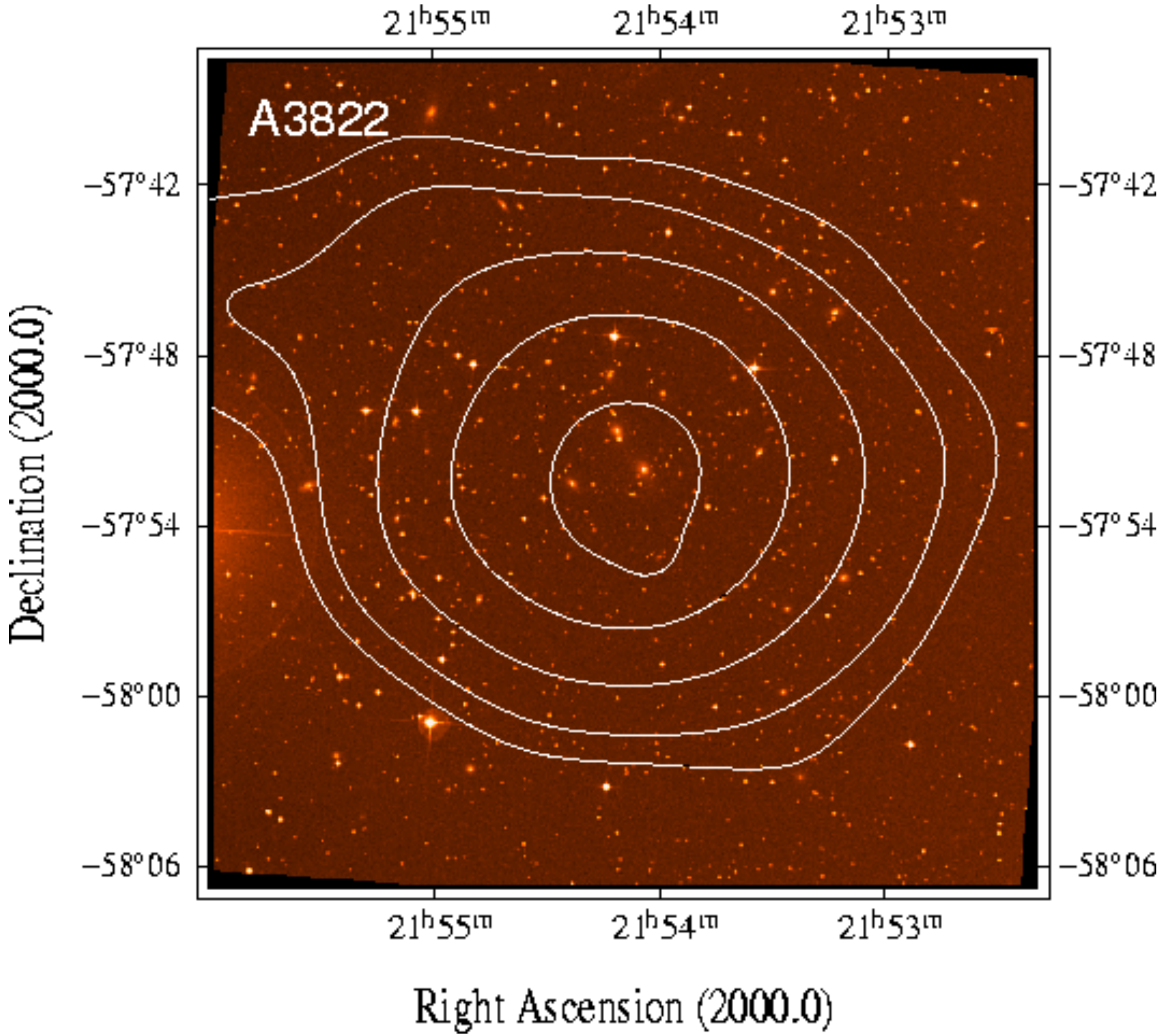

Reiprich ApJ, 567, 716-740 (2002)

Bremsstrahlung

Gas falling into clusters shock heats to the virial temperature of the potential, kT ~ mV^2 resulting in an intracluster medium (ICM) composed of hot plasma. This plasma radiates in X-rays via Bremsstrahlung (braking radiation). [Sometimes also called free-free radiation]
Just classical radiation from accelerated charges.

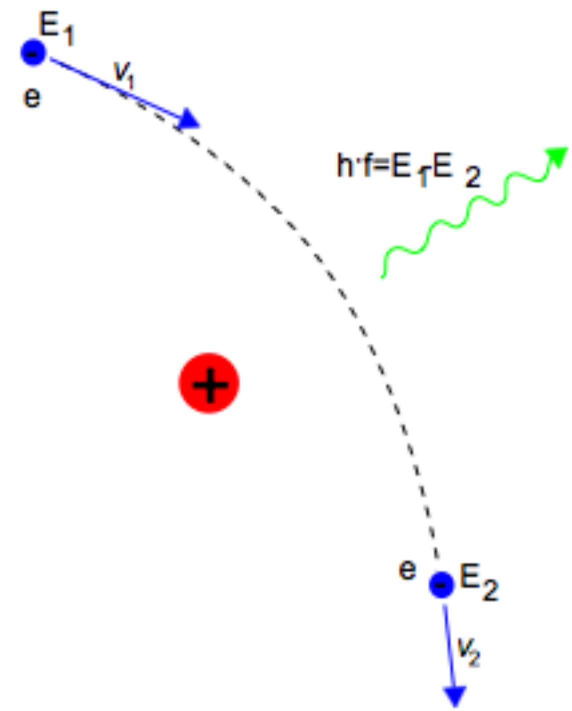

Global correlations in galaxy clusters

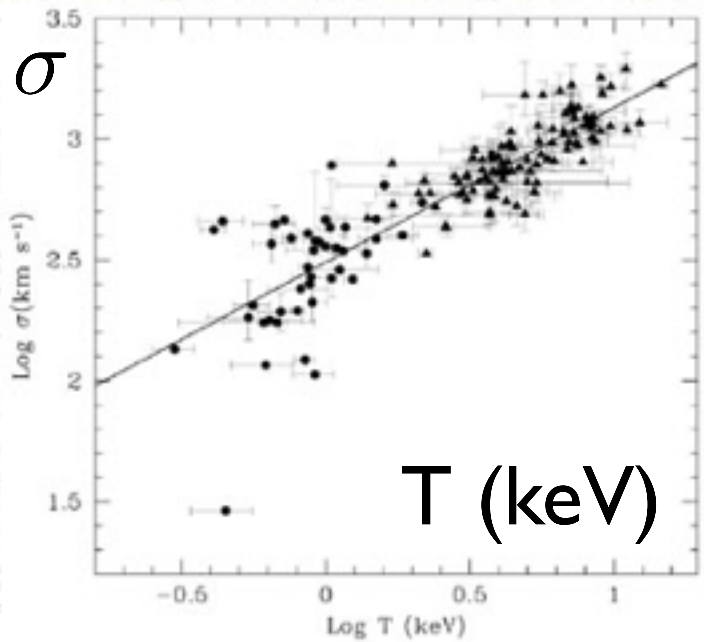

Figure 4. Logarithm of the X-ray temperature versus logarithm of optical velocity dispersion for a sample of groups (circles) and clusters (triangles). The group data are taken from the literature compilation of Xue & Wu (2000), with the addition of the groups in Helsdon & Ponman (2000). The cluster data are taken from Wu et al (1999). The solid line represents the best-fit found by Wu et al (1999) for the clusters sample (using an orthogonal distance regression method). Within the large scatter, the groups are consistent with the cluster relationship.

Mulchaey *Annu. Rev. Astron. Astrophys. 2000. 38: 289*

Global correlations in galaxy clusters

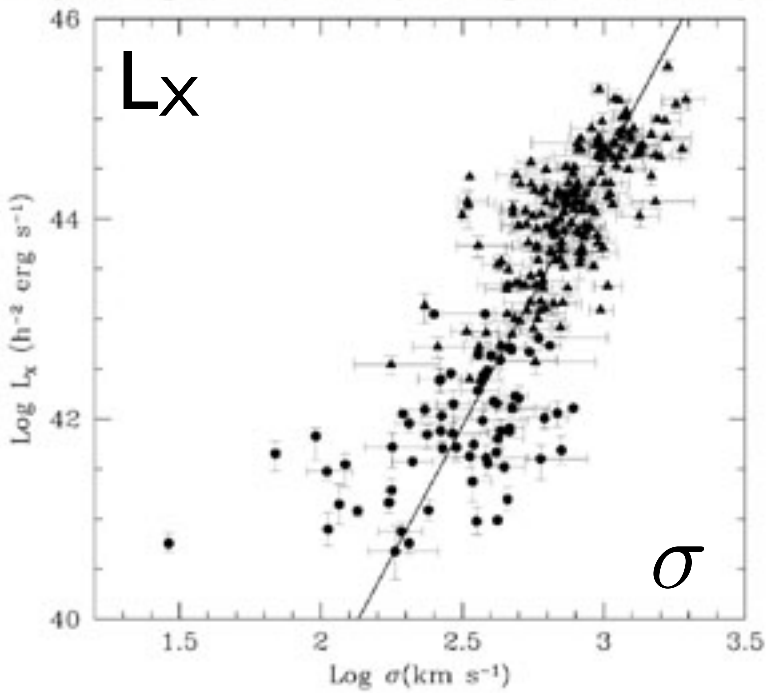

Figure 5. Logarithm of optical velocity dispersion versus logarithm of X-ray luminosity for a sample of groups (circles) and clusters (triangles). The data are taken from the same sources cited in Figure 4. The solid line represents the best-fit found by Wu et al (1999) for the clusters sample (using an orthogonal distance regression method).

Mulchaey *Annu. Rev. Astron. Astrophys. 2000. 38: 289*

Global correlations in galaxy clusters

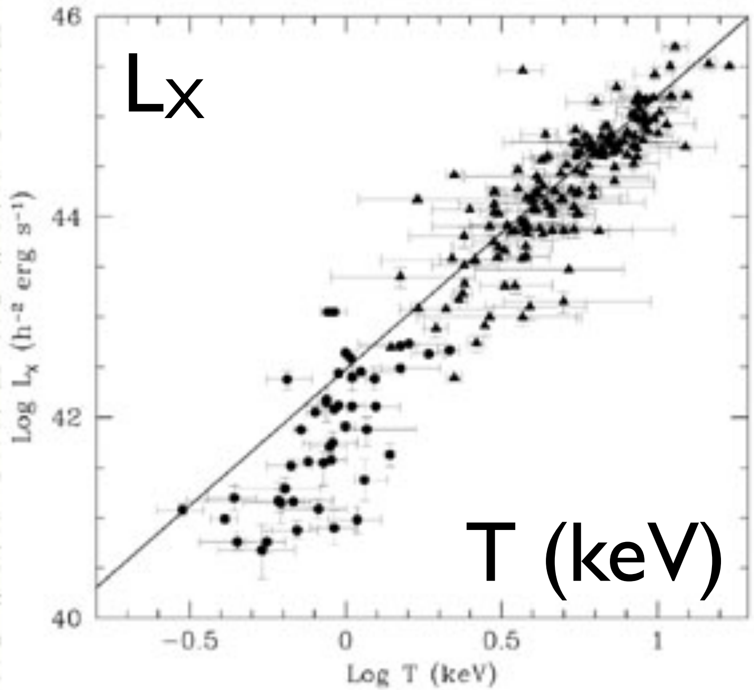

Figure 6. Logarithm of the X-ray temperature versus logarithm of X-ray luminosity for a sample of groups (circles) and clusters (triangles). The data are taken from the same sources cited in Figure 4. The solid line represents the best-fit found by Wu et al (1999) for the clusters sample (using an orthogonal distance regression method). The observed relationship for groups is somewhat steeper than the best-fit cluster relationship.

Mulchaey *Annu. Rev. Astron. Astrophys. 2000. 38: 289*

Beta models

The X-ray surface brightness at a projected radius R

for an isothermal sphere is given by:

$$S(R) = S_0[1 + (R/r_c)^2]^{-3\beta+1/2}$$

S_0 central surface brightness

r_c core radius of gas distribution

$$\beta \equiv \frac{\mu m_p \sigma^2}{kT_g} = \frac{\text{specific energy in galaxies}}{\text{specific energy in the hot gas}}$$

$$\beta \equiv \frac{\mu m_p \sigma^2}{kT_g} = \frac{\text{specific energy in galaxies}}{\text{specific energy in the hot gas}}$$

μ is the mean molecular weight

m_p is the mass of the proton

σ is the one-dimensional velocity dispersion of the galaxies

T_g is the temperature of the ICM

Typically the gas is assumed to be isothermal

β treated as fit parameter; typically ~ 2/3
BUT often higher when sigma well measured
and often lower in groups

Mass Estimator

$$M_{tot}(< R) = \frac{kT_g(R)}{G\mu m_p}\left[\frac{\partial \log \rho}{\partial \log r} + \frac{\partial \log T}{\partial \log r}\right] R$$

the gas density profile is determined by fitting the standard beta model to the surface brightness profile.

the gas temperature is measured directly from the X-ray spectrum

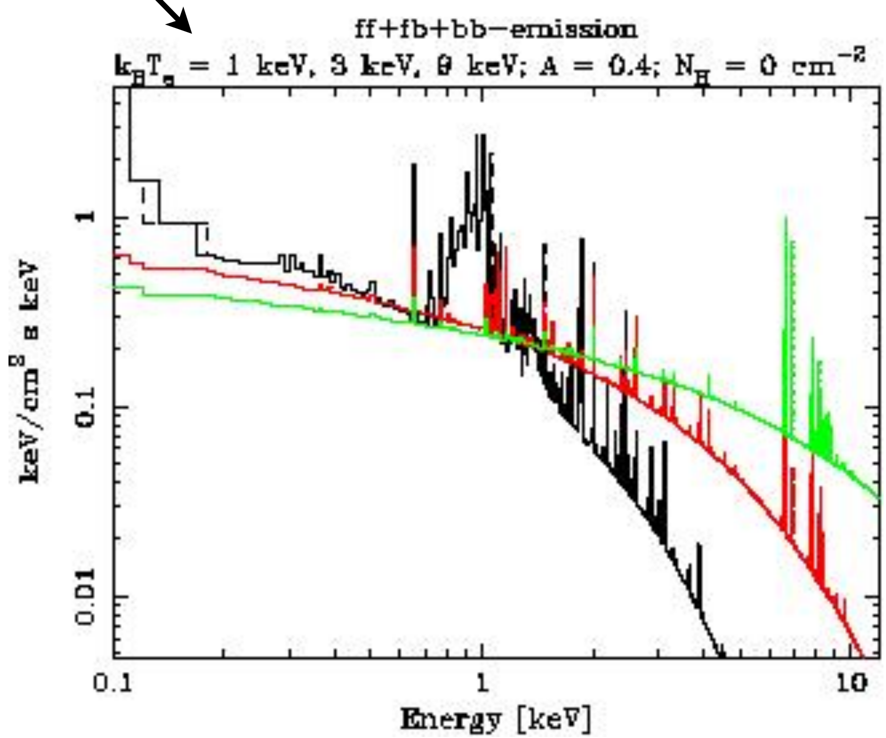

Assumes
- hydrostatic equilibrium
- sphericity

often assumes
- isothermality → $\frac{\partial \log T}{\partial \log r} = 0$

Mass Estimator

$$M_{tot}(< R) = \frac{kT_g(R)}{G\mu m_p}\left[\frac{\partial \log \rho}{\partial \log r} + \frac{\partial \log T}{\partial \log r}\right] R$$

basically,

$$M_{tot}(< R) \sim T_{gas}\, R$$

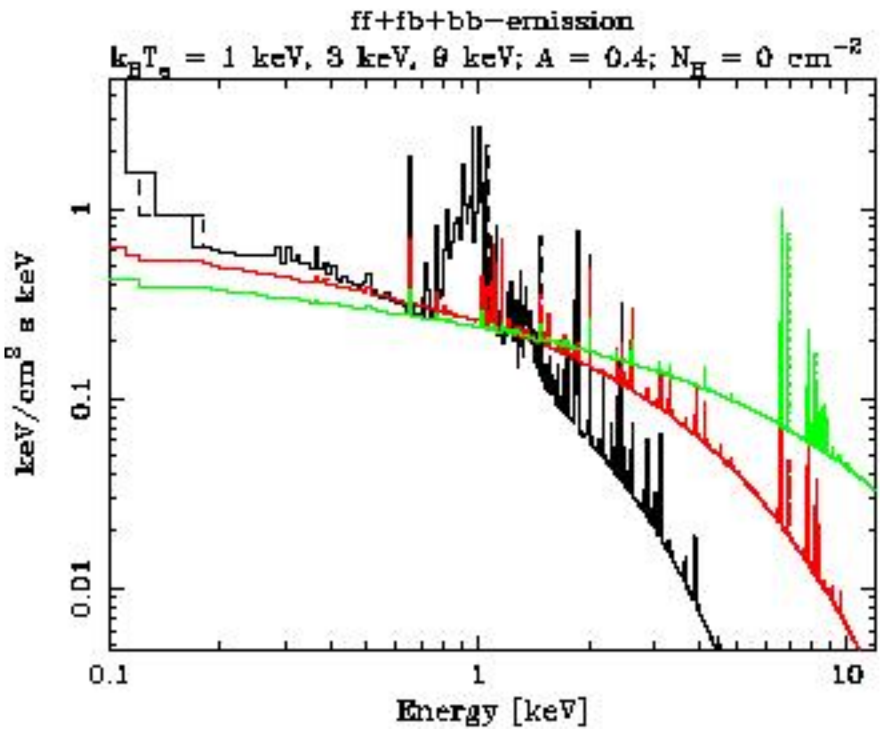

Rasheed (2010)

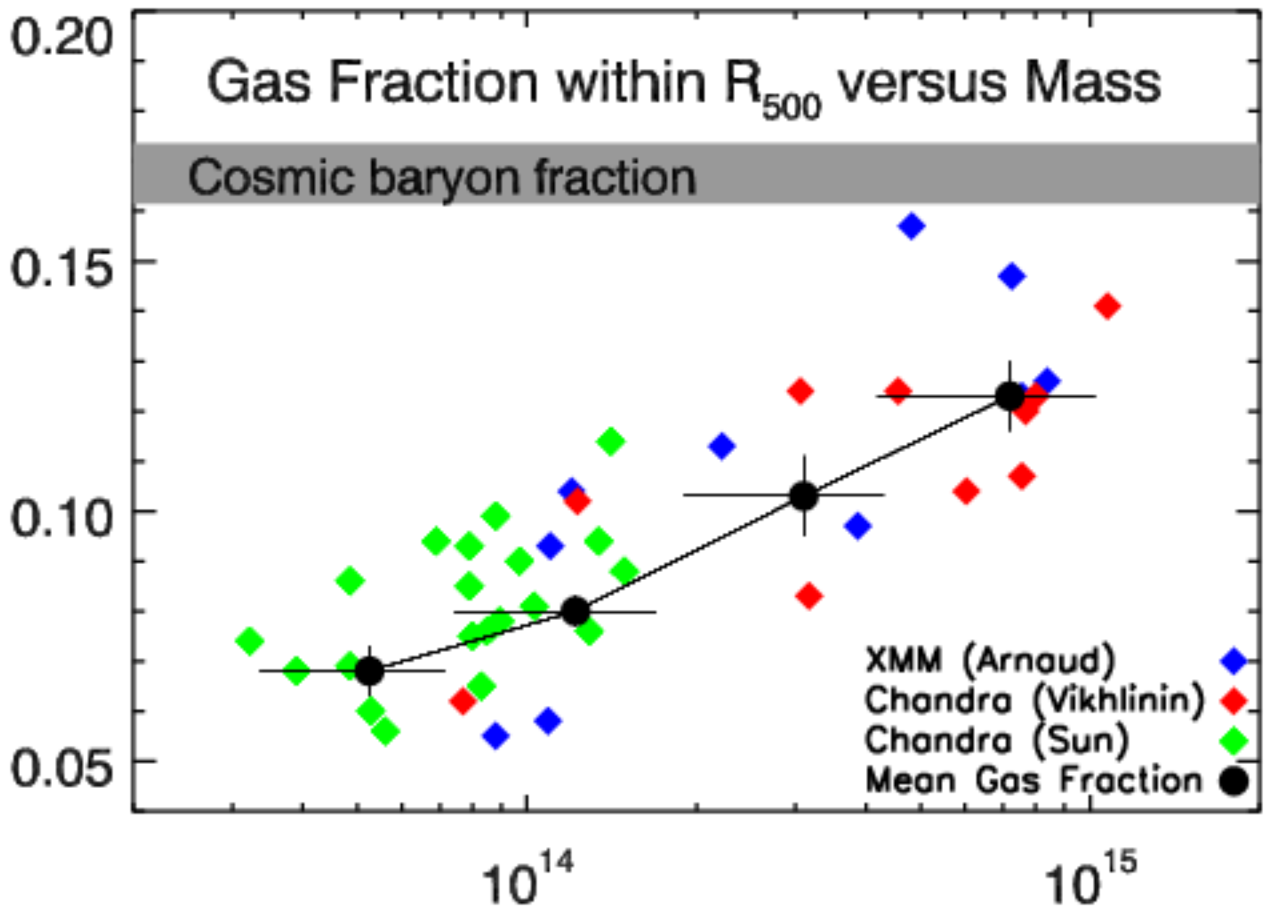

Typical result:

clusters have close to, but not quite, expected baryon fraction

Rasheed (2010)

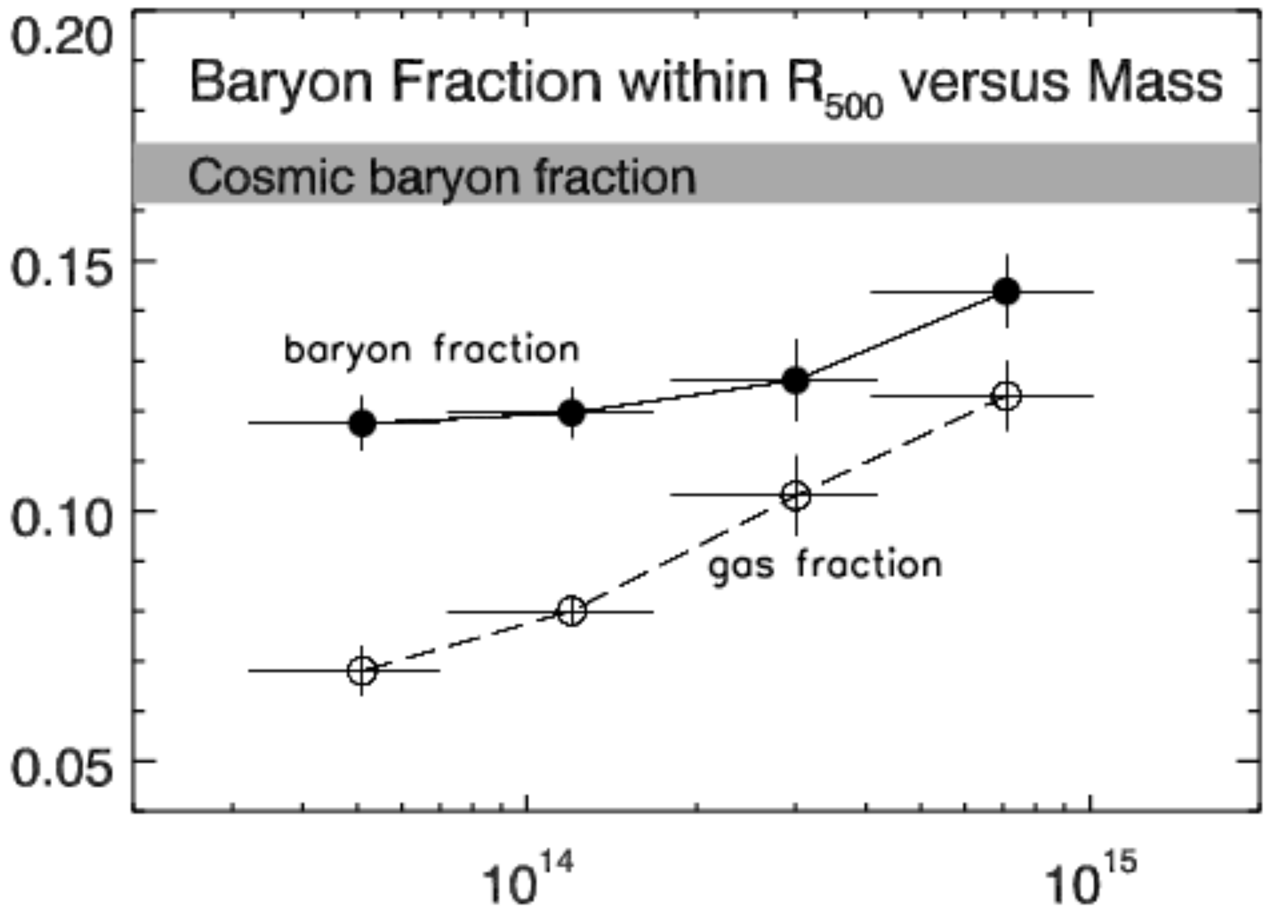

Typical result:
clusters have progressively more gas than stars at higher masses

Rasheed (2010)

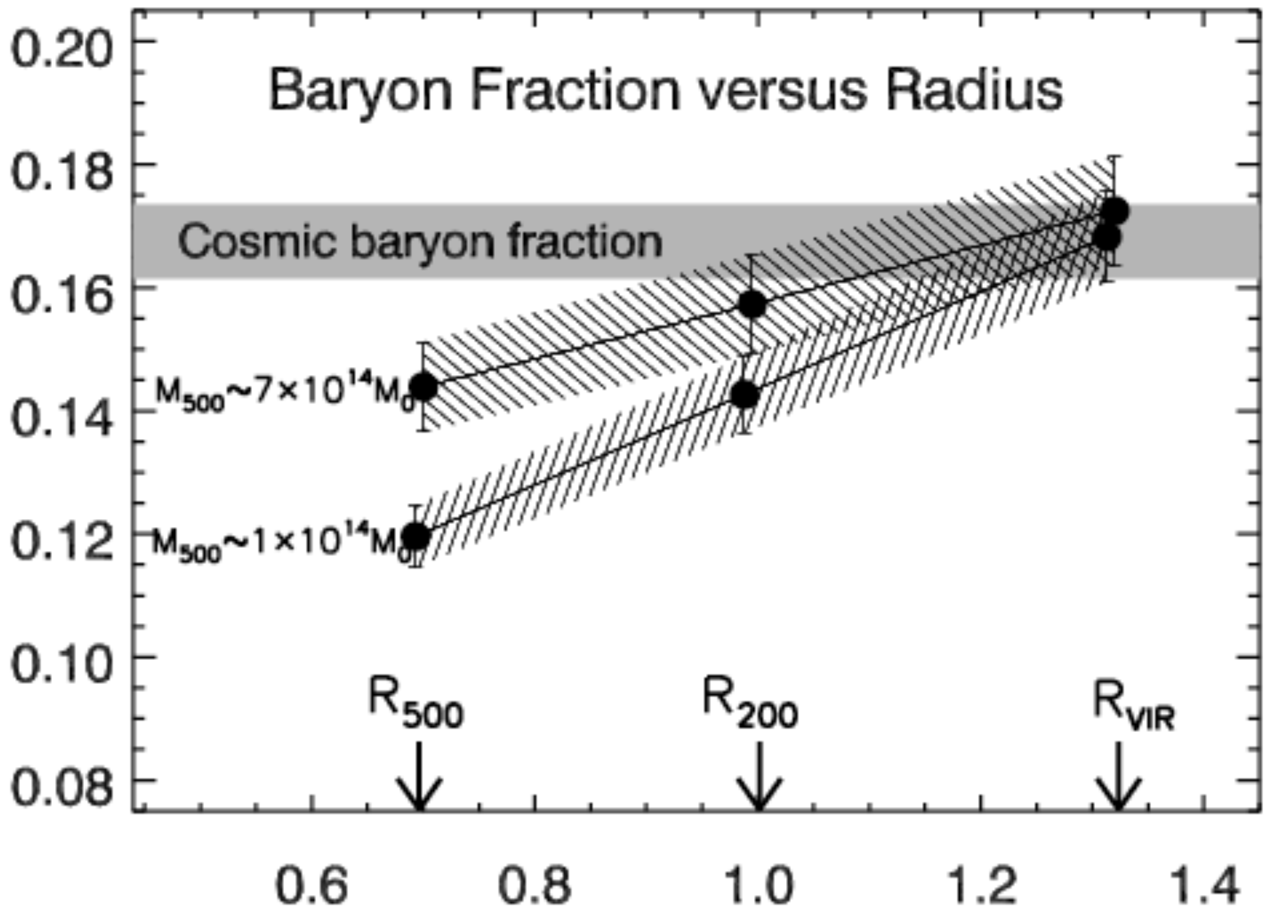

Typical result:
the baryon fraction increases with radius

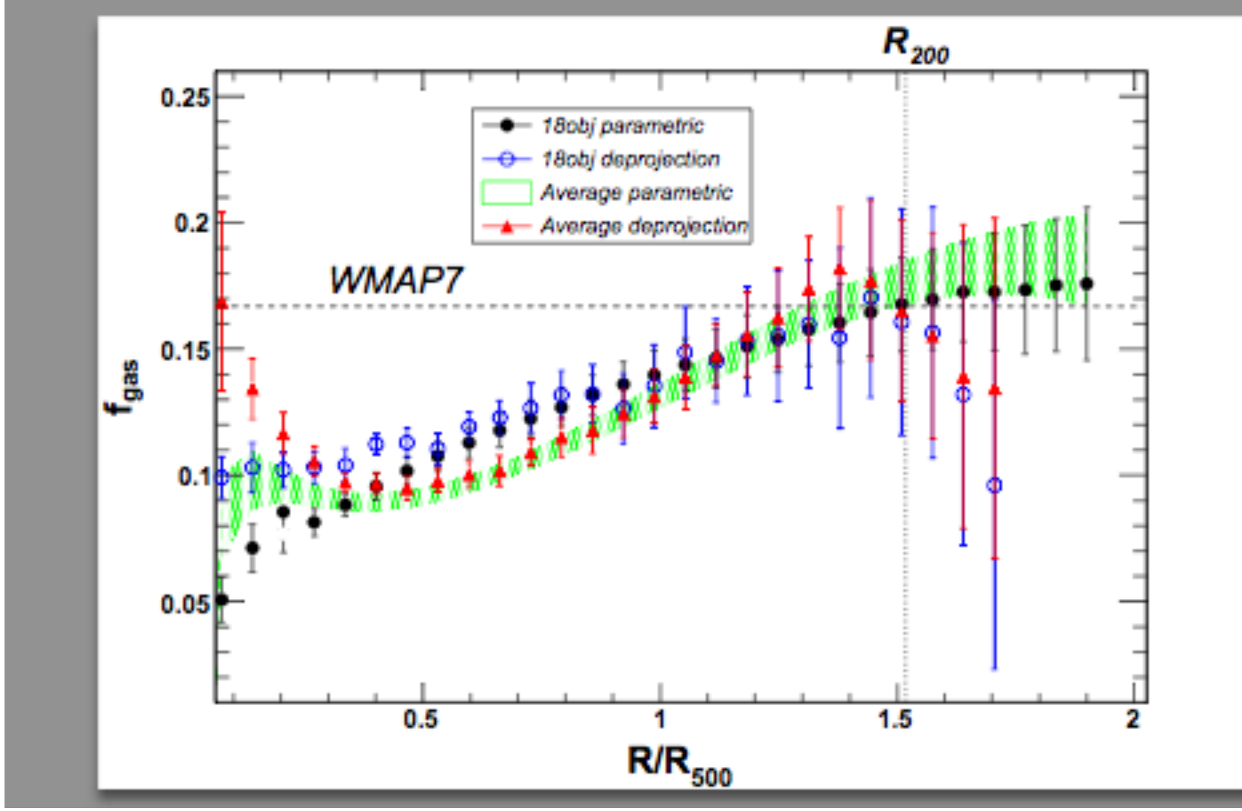

Typical result:
ICM gas outweighs the stars by factor of ~6;
outweighed by dark matter be same factor

there seems to be more dark matter towards the centers of clusters

SUNYAEV–ZEL'DOVICH EFFECT

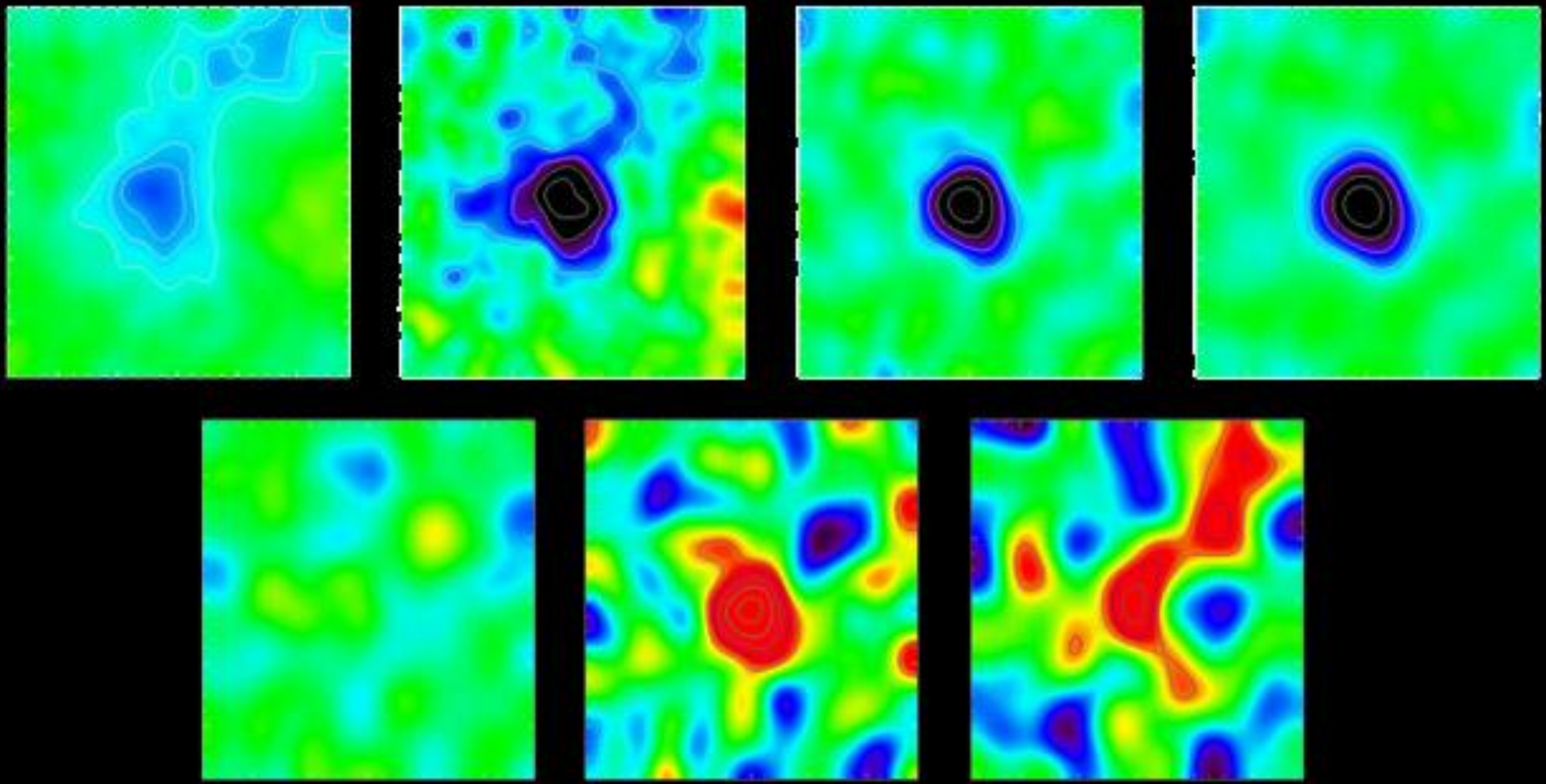

SUNYAEV–ZEL'DOVICH EFFECT

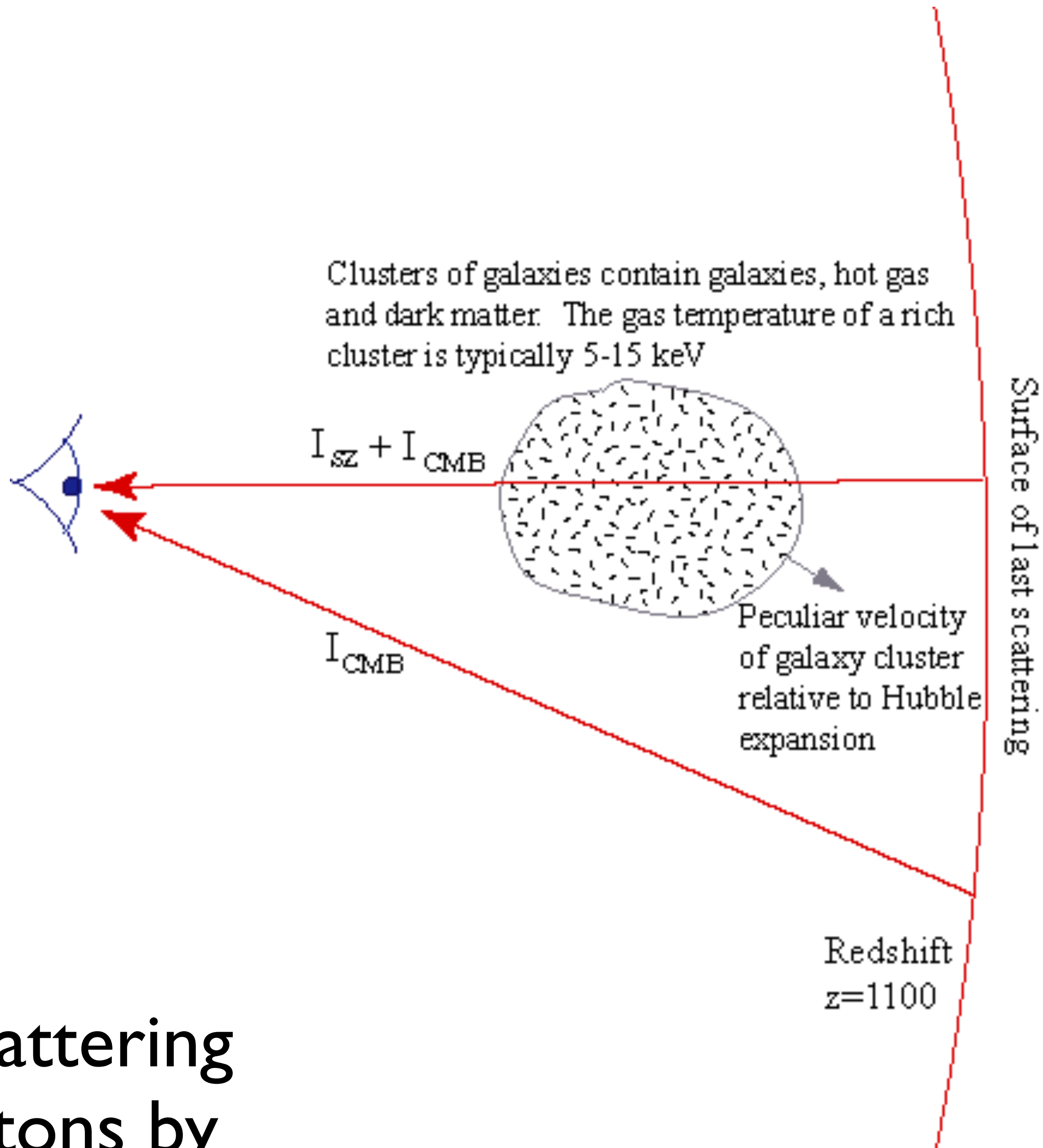

Compton scattering of CMB photons by hot ICM plasma frequency dependent change in intensity

$$\frac{\delta I_{nu}}{I_\nu} = -y\frac{xe^x}{e^x - 1}\left[4 - x\coth\left(\frac{x}{2}\right)\right]$$

where $x = \frac{h\nu}{kT_{rad}}$ and $y = \int \sigma_T n_e \frac{kT_g}{m_e c^2} d\ell$

CMB (T_{rad})

electron density (n_e)

Thomson scattering cross-section (σ_T)

y is the Compton y-parameter which quantifies how much effect the plasma has frequency dependent change in intensity

$$\frac{\delta I_{nu}}{I_\nu} = -y \frac{x e^x}{e^x - 1} \left[4 - x \coth\left(\frac{x}{2}\right)\right]$$

where $x = \dfrac{h\nu}{kT_{rad}}$ and $y = \displaystyle\int \sigma_T n_e \frac{kT_g}{m_e c^2} d\ell$

at low frequency in the Rayleigh-Jeans tail,

$$\frac{\delta I}{I} = \frac{\delta T}{T} = -2y$$

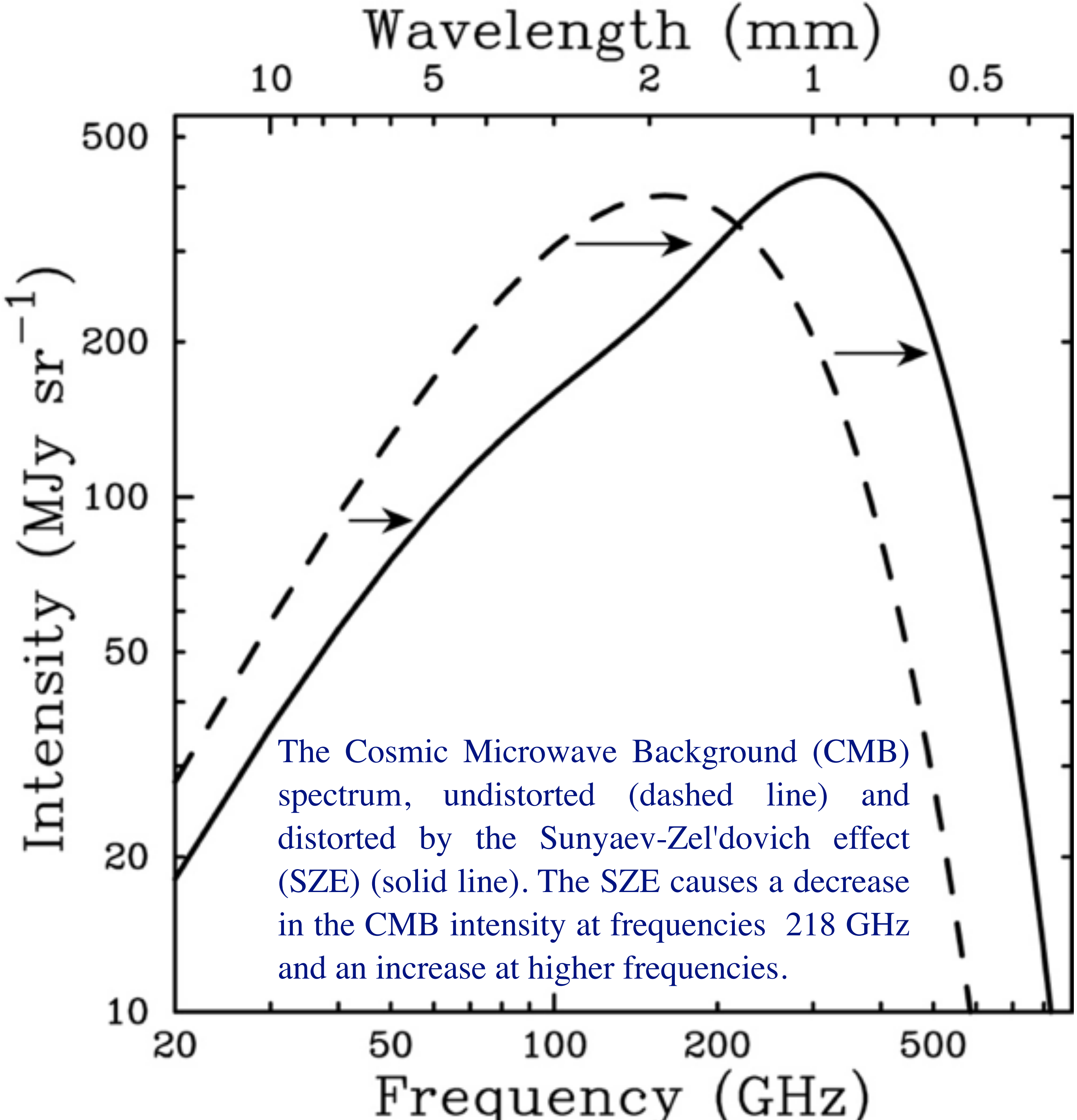

The Cosmic Microwave Background (CMB) spectrum, undistorted (dashed line) and distorted by the Sunyaev-Zel'dovich effect (SZE) (solid line). The SZE causes a decrease in the CMB intensity at frequencies 218 GHz and an increase at higher frequencies.

Carlstrom et al. Annu. Rev. Astron. Astrophys. 2002. 40: 643

Thermal SZ effect from Compton scattering of CMB photons by cluster plasma

intensity boosted

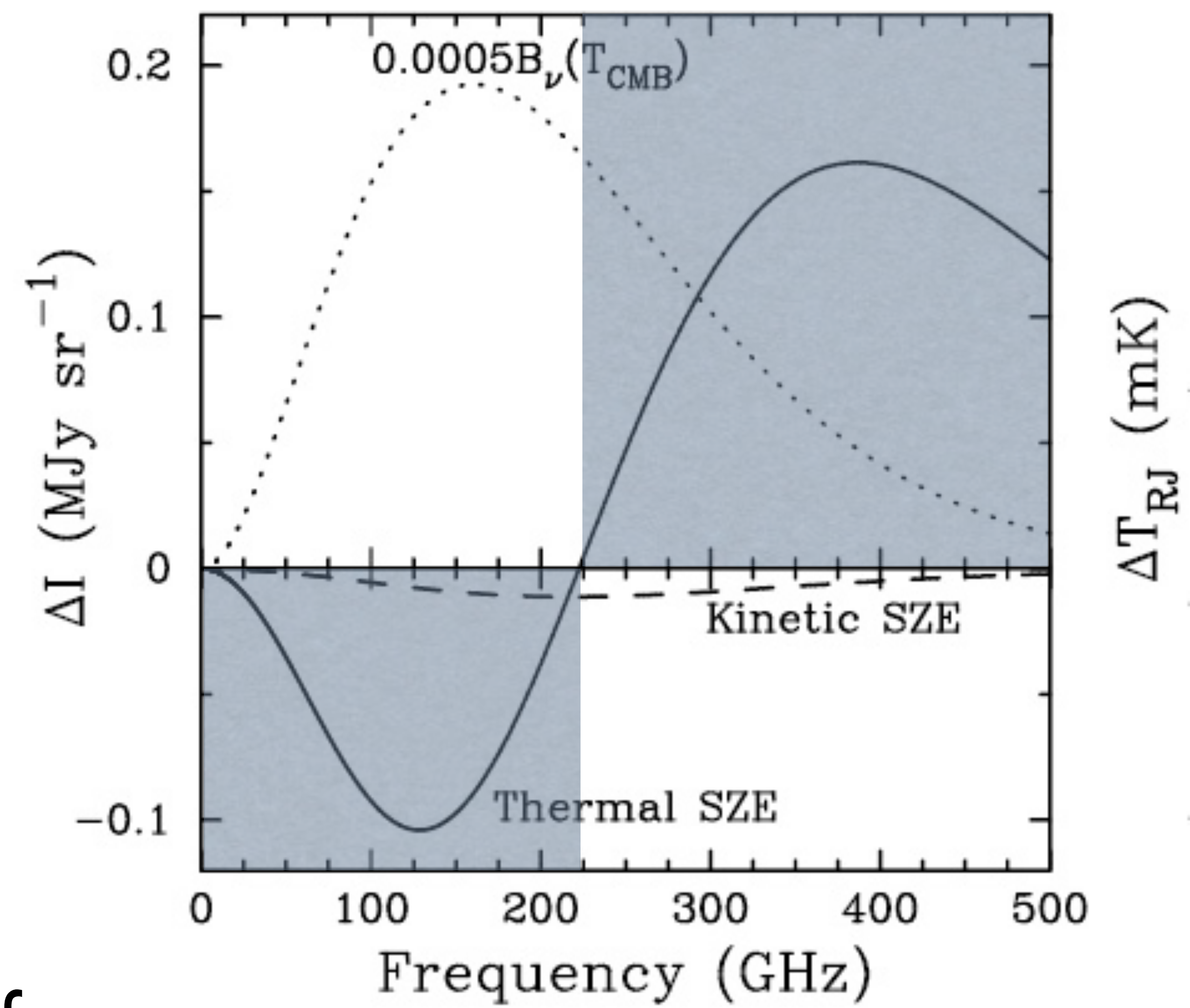

Kinematic SZ effect from peculiar velocity of cluster wrt CMB frame

intensity depleted

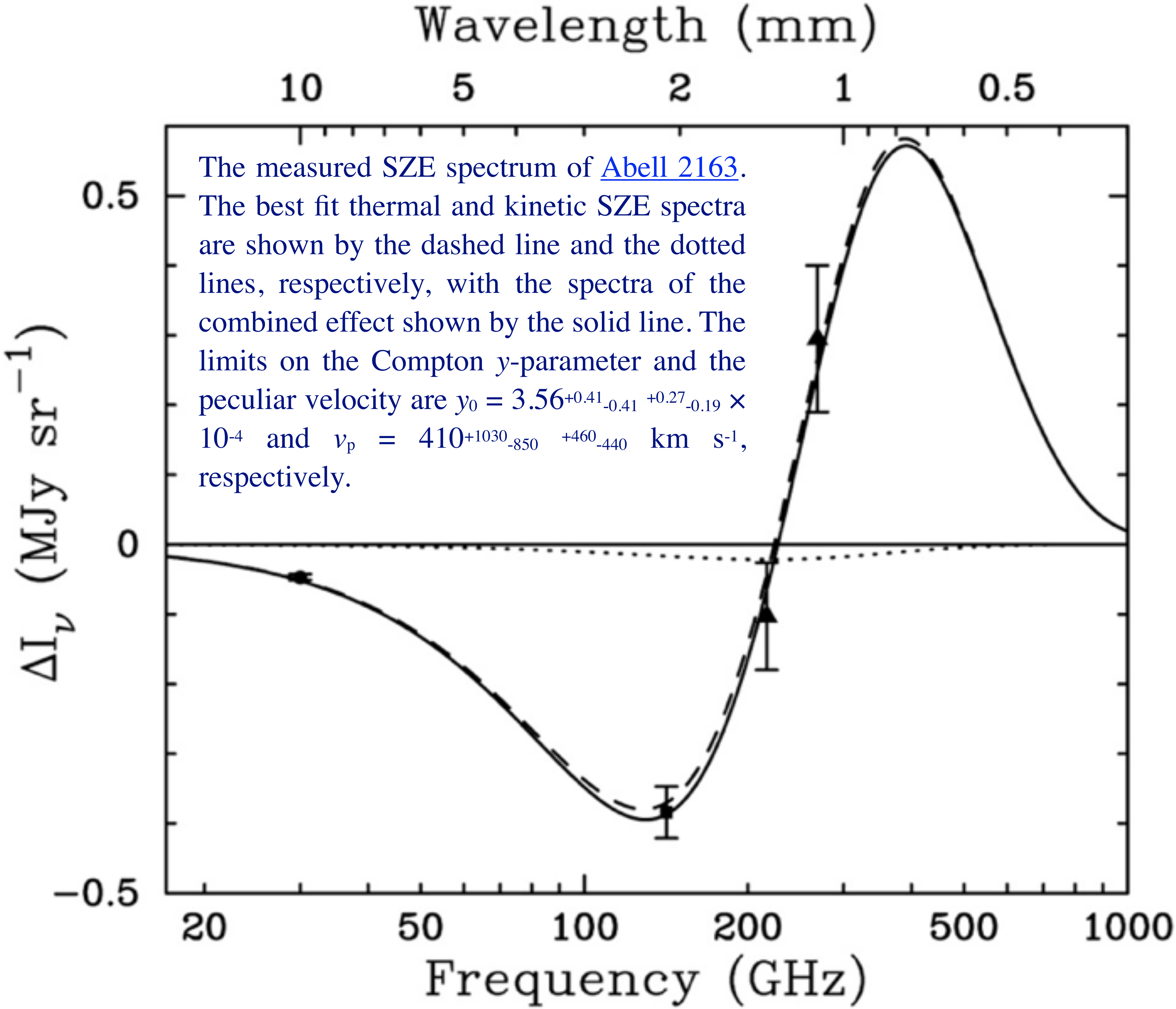

The measured SZE spectrum of Abell 2163. The best fit thermal and kinetic SZE spectra are shown by the dashed line and the dotted lines, respectively, with the spectra of the combined effect shown by the solid line. The limits on the Compton *y*-parameter and the peculiar velocity are $y_0 = 3.56^{+0.41}_{-0.41}{}^{+0.27}_{-0.19} \times 10^{-4}$ and $v_p = 410^{+1030}_{-850}{}^{+460}_{-440}$ km s^{-1}, respectively.

SUNYAEV–ZEL'DOVICH EFFECT

detected by Planck

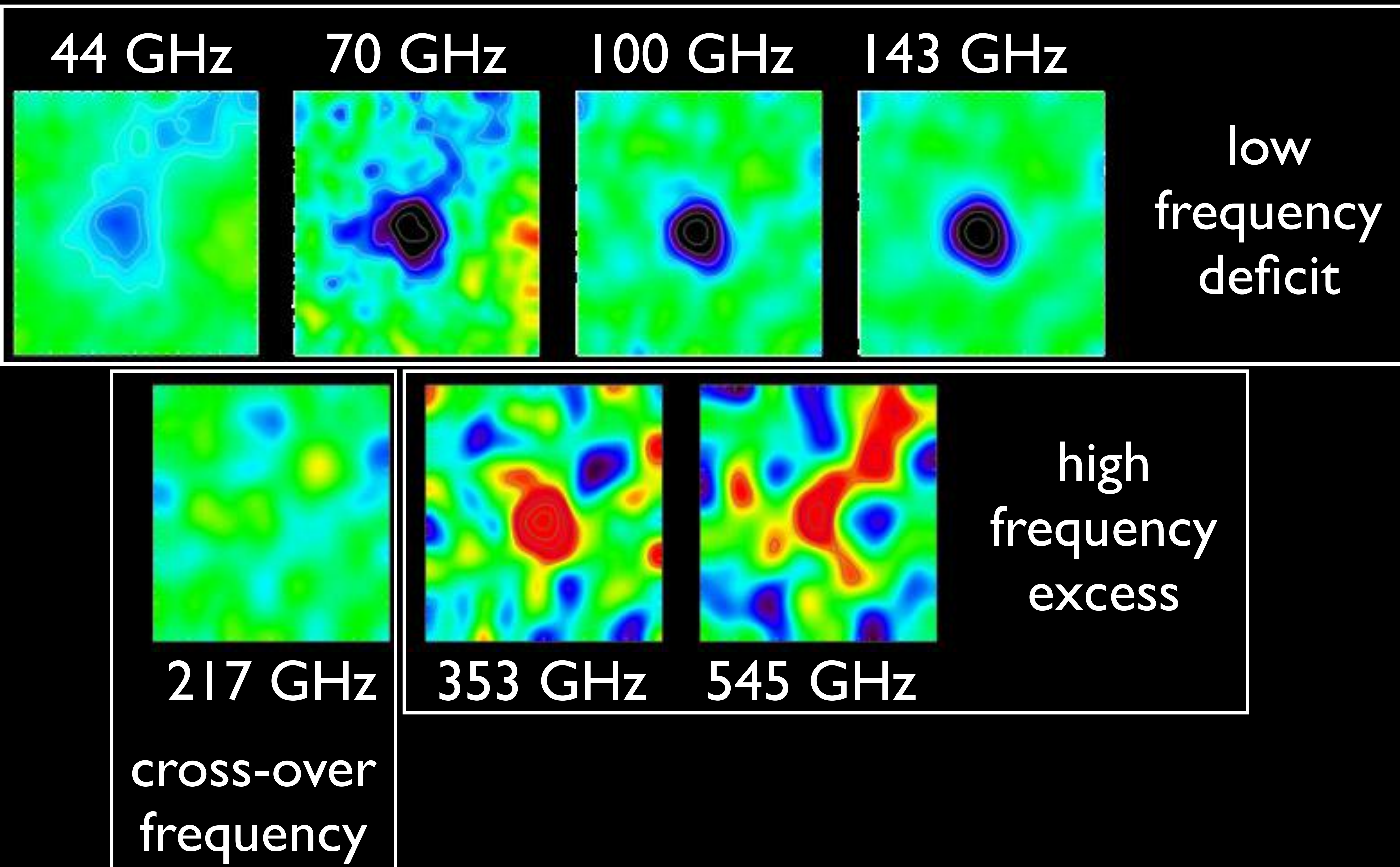

integrated change in CMB temperature

$$\int \Delta T d\Omega \propto \frac{N_e \langle T_e \rangle}{D_A^2} \propto \frac{M \langle T_e \rangle}{D_A^2}$$

depends on the total number of electrons, their temperature, and the area they subtend on the sky. In effect measures Pressure, or mass if T known.

D_A is the angular diameter distance.
At high z, it varies slowly, while the density increases as $(1+z)^3$

... SZ effect weak, but nearly independent of redshift!